

Imaging Techniques in CKD-MBD

Subjects: [Radiology](#), [Nuclear Medicine & Medical Imaging](#)

Contributor: Pablo Ureña-Torres

Standard radiological imaging is generally used for the diagnosis of fracture or pseudo-fractures, vascular calcifications and other features of CKD-MBD. However, bone fractures can also be diagnosed using computed tomography (CT) scan, magnetic resonance (MR) imaging and vertebral fracture assessment (VFA). Fracture risk can be predicted by bone densitometry using dual-energy X-ray absorptiometry (DXA), quantitative computed tomography (QTC) and peripheral quantitative computed tomography (pQTC), quantitative ultrasound (QUS) and most recently magnetic resonance micro-imaging.

bone

fracture

bone mineral density

computed tomography

cortical bone

trabecular bone

CKD-MBD

dual-energy X-ray absorptiometry

1. Introduction

The mineral and bone disorders associated with chronic kidney disease (CKD) are often progressive in earlier stages of CKD but remain clinically silent until stages G3b-G4 (estimated glomerular filtration rate (eGFR) 30 to 44 or 15 to 29 mL/min/1.73 m² of body surface). Serum bone biomarkers are the earliest indicators of mineral bone diseases (MBD) during CKD progression, starting with decreased circulating alpha klotho levels and an increase of serum fibroblast growth factor 23 (FGF23). As CKD progresses, circulating 1,25 dihydroxyvitamin D values decrease, serum parathyroid hormone (PTH) rises and subsequent detectable alterations of serum calcium and phosphate metabolism occur [\[1\]](#). The prevalence of CKD is still growing above other life-style diseases, affecting over 850 million people worldwide [\[2\]](#), and as patients get older and have a longer life expectation, the prevalence of CKD rises, together with the incidence of MBD. The combination of CKD-related low or high rates of bone turnover, mineralization defects and reduced bone mass has been termed renal osteodystrophy. However, seen more globally, bone disease in CKD is the sum of CKD-specific risk factors, which are in turn dependent on CKD progression, together with age- or sex-related bone loss. These complex and interacting changes to bone require careful evaluation, including using imaging techniques [\[3\]](#).

2. Characteristics of Bone Structure

Eighty percent of the human skeleton is composed of cortical bone and the other 20% is trabecular bone [\[4\]](#). The proportion of cortical and trabecular bone differs according to each skeletal site, so the information provided by imaging should be considered in the light of this distribution. When evoked by pain, imaging techniques offer

guidance towards the type of CKD-MBD and may reveal prevalent fractures or pseudo-fractures. Imaging can also provide information on bone fragility and monitor changes after a medical intervention.

Due to its higher proportion of cortical bone, imaging of the proximal femur or femoral neck sites reflect more accurately cortical BMD, which is correlated to femoral strength. With age, cortical bone resorption accelerates, resulting in cortical thinning and increased cortical porosity. Chronic metabolic changes such as high PTH in CKD patients further enhance these features.

3. Bone and Soft Tissue Imaging

Plain radiographs do not quantify bone loss, and consequently other techniques

Table 1. Different imaging techniques, underlying lesion mechanisms and localization and CKD stage in which it is mostly used.

Type	Mechanism	Skeletal Site	Type of Bone Disease	CKD Stage
Plain Radiography	Bone resorption lesions Bone cysts Fractures	Sub-periosteal Subchondral Sub-tendinous Extra-skeletal calcifications All skeleton	Secondary Hyperparathyroidism Multiple Myeloma Amyloidosis Osteonecrosis Osteoporosis Calcific Uremic Arteriopathy	All
DXA	Areal BMD measurements	Hip, distal radius, lumbar spine, whole body	Osteopenia Osteoporosis	All
Vertebral Assessment Fracture (VAF)	Vertebral deformities	Spine	Vertebral fractures	All
HR-pQCT	Trabecular architecture Volumetric BMD	Hip, distal radius, distal tibia	Secondary Hyperparathyroidism	All and research
Bone Scintigraphy	Tracer accumulation occurs in osteoblastic activity, and to a lesser extent, skeletal vascularity; Systemic amyloid burden;	Whole body	Osteoarthritis Metabolic Bone Disease: -Hyperparathyroidism and vitamin D deficiency -Osteomalacia; Fractures Enthesopathies Osteonecrosis Rare Osteoarticular Diseases: Sarcoidosis with bone involvement;	3–5

Type	Mechanism	Skeletal Site	Type of Bone Disease	CKD Stage
			Amyloidosis: ¹²³ I SAP scintigraphy if available—assess amyloid deposition in liver, spleen, kidneys, adrenals, localized soft tissue deposits and bones ¹³¹ I-β2M amyloidosis	
MRI	Cortical porosity Marrow fat content and composition Marrow perfusion, and molecular diffusion	Distal radius, distal tibia, calcaneus, hip, spine Whole skeleton	Secondary Hyperparathyroidism	Research
PET	Bone formation rate, osteoclast, osteoblast, erosion and mineralized surfaces	Lumbar region	Low or high bone turnover disease	All
US	Cortical deterioration	Tibia	Secondary Hyperparathyroidism	Research

DXA, Dual-energy X-ray Absorptiometry; BMD, Bone Mineral Density; HR-pQCT, High Resolution-peripheral Quantitative Computerized Tomography; MRI, Magnetic Resonance Image; PET, Positron Energy Tomography; US, Ultrasounds Velocity.

have been developed such as radiographic absorptiometry, DXA, QUS, QCT, pQCT, HR-pQCT and more recently quantitative magnetic resonance imaging (MRI). These methods facilitate an analytic approach and may improve the distinction between differing bone pathologies and fracture prediction in patients with CKD. The main limitation is the affordability of some methods, and the need for validation in CKD populations before being suggested its use in clinical practice ([Table 1](#)).

3.1. Conventional Radiography

Radiography is widely available, affordable and the most used radiological imaging method to characterize bone disease, including specific features of CKD ([Figure 1](#)). Plain x-rays can provide information about high bone remodeling and mineralization failure.



Figure 1. Standard Skeletal Radiography images: (A) Left lower arrow, sub periosteal resorption of the distal phalanx of the middle finger, and at the intermediate phalanx of the index finger as indicated by the right upper arrow in a hemodialysis patient, virtually pathognomonic of severe secondary hyperparathyroidism. (B) Image of a “brown tumor” at the distal radius metaphyseal as indicated by the arrow. It is a well-limited lytic lesion with endosteal scalloping, one of the possible manifestations of severe secondary hyperparathyroidism. (C) Periarticular calcifications of the glenohumeral ligaments, appearing as cloud-like densities that diffuse into the adjacent tenosynovial tissues. (D) “Salt and pepper” aspect of the calvaria seen as well-defined lucencies suggesting bone resorption. (E) Lateral spine X-ray can be used to assess vertebral fracture in a hemodialysis patient. (F) Multiple oblique spiral fractures in the proximal, middle and distal third of the humerus in a hemodialysis patient with osteomalacia.

Osteosclerosis is an additional feature of SHPT occurring predominantly in the axial skeleton and often detected on lateral lumbar spine radiographs [5] affecting the superior and inferior endplates (“ruger jersey spine”), this is mostly due to deposition of mineral crystals and calcification in the collagenous portion of the endplates. Conventional x-rays also identify extra-skeletal calcifications. Plain radiographs may also reveal the now rare entity of amyloid arthropathy, characterized by subchondral erosions [6], often located in periarticular bone and at the site of ligamentous insertions [7].

3.2. Dual-Energy X-ray Absorptiometry

DXA is valuable for the quantification of BMD and the evaluation of fracture risk [8]. Axial measurement of the lumbar spine and hip (central DXA) using a stationary scan table is the most common modality. The technique produces little radiation and obtains a rapidly acquired two-dimensional (areal) image with good resolution.

3.3. DXA-Derived Trabecular Bone Score (TBS)

The trabecular bone score (TBS) is another available and validated tool that evaluates trabecular microarchitecture through BMD measures obtained at the lumbar spine by DXA [9]. An advantage of TBS is that overlapping vascular calcifications and degenerative changes do not interfere with its measurement. Patients on hemodialysis have a significantly lower TBS than controls without osteoporosis, and this is independent of BMD or other covariates (1.15 ± 0.181 vs. 1.32 ± 0.123 , $p = 0.001$, respectively) [10].

3.4. Radiographic Absorptiometry (RA)

DXA and TBS techniques may not be widely available because of their relatively high capital cost and lack of expertise in many non-industrialized countries. In this case, RA could be an alternative approach for the evaluation of BMD. RA is both rapid and inexpensive because it does not require dedicated equipment. RA measures the second metacarpal mid-shaft BMD by using X-ray radiographs, combined with digital image processing (DIP) and a computed X-ray densitometer to improve the precision and accuracy [11][12]. Several studies have shown that RA-based BMD assessment can reliably be used for the estimation of fracture risk in post-menopausal women [13]. In hemodialysis patients, a recent study in 456 hemodialysis patients demonstrate that lower metacarpal BMD measured by DIP-assisted RA predicts the risk of osteoporotic fractures [14].

3.5. Quantitative Computerized Tomography

QCT allows in vivo assessment of trabecular architecture, volumetric BMD and bone size, from which BMD can be estimated. QCT also provides a functional approach to bone densitometry by measuring bone strength through biomechanical parameters. QCT imaging can disclose pathological fractures and delineate joint lesions related to amyloidosis. As QCT uses a high radiation dose in a small field of view, it can also be used to monitor bone structural changes over time, disease progression and treatment efficacy. However, In vivo applications are limited. Peripheral QCT (pQCT) limits radiation to the tibia and distal radius.

3.6. High Resolution-Peripheral Quantitative Computerized Tomography (HR-pQCT)

HR-pQCT provides excellent spatial resolution, differentiating trabecular from cortical bone and using a lower radiation dose (Figure 2).

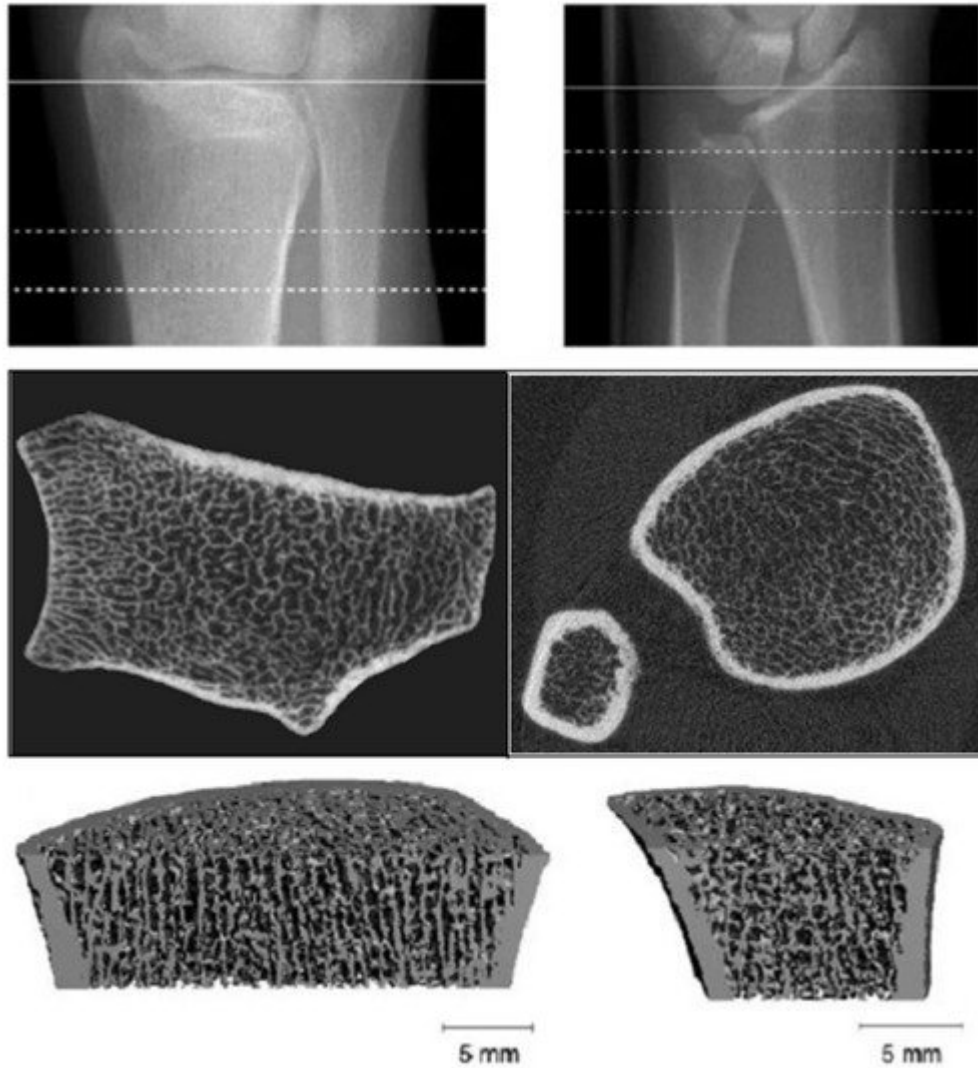


Figure 2. High resolution-peripheral quantitative computerized tomography (HR-pQCT): Analysis of trabecular and cortical microarchitecture proximally and distally at ulnar and radial level.

3.7. Magnetic Resonance Imaging (MRI)

Whereas HR-pQCT is more limited to peripheral skeleton regions like the radius and tibia, MRI can also image sites such as the proximal femur, but usually with lower spatial resolution ([Figure 3](#)).

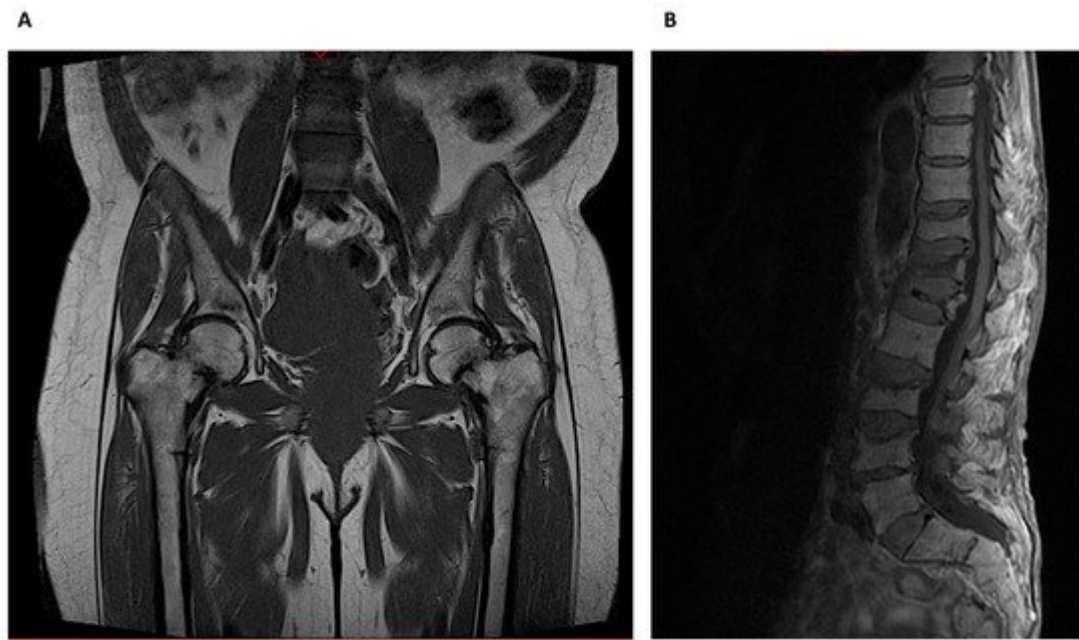


Figure 3. Magnetic Resonance Imaging: (A) Bilateral metaphyseal femoral fractures distal to the lesser trochanter with reactionary associated bone edema in a hemodialysis patient with osteomalacia. (B) Osteoporotic lumbar spine compression fracture at T11, T12, L1, L3 and L4 vertebral body that is hyperintense on T2 and shows vivid contrast enhancement with paravertebral soft tissue edema.

3.8. Other Imaging Techniques

Nuclear imaging techniques based on radiotracer accumulation can be used for determining the extent, progression and for monitoring of systemic diseases. Positron energy tomography (PET) scanning is a noninvasive quantitative imaging technique that estimates bone turnover [15] through the measurement of fluoride activity in the bone. Bone formation rate [16], osteoclast, osteoblast, erosion and mineralized surfaces correlate with the tracer intake. PET was superior to PTH in differentiating patients with low from high bone turnover in 26 hemodialysis patients [15]. Ultrasound (US) velocity at the tibia was found to be significantly lower in 42 hemodialysis patients when compared to the control group indicating cortical deterioration related to the degree of SHPT [17]. More studies are needed to validate US as a screen and diagnosis tool regarding the evaluation of CKD-MBD.

Finally, HR-MRI, Raman spectroscopy, Fourier transform infrared spectroscopy, and quantitative backscatter electron imaging [18] are also currently being used in research studies. To date, none of these techniques can be recommended for use in clinical care.

References

1. Isakova, T. An Introduction to PTH, Phosphate and Vitamin D: Current Issues and Concerns. *Semin. Dial.* 2015, 28, 563.

2. Jager, K.J.; Kovesdy, C.; Langham, R.; Rosenberg, M.; Jha, V.; Zoccali, C. A single number for advocacy and communication—worldwide more than 850 million individuals have kidney diseases. *Kidney Int.* 2019, 96, 1048–1050.
3. Covic, A.; Vervloet, M.; Massy, Z.A.; Torres, P.U.; Goldsmith, D.; Brandenburg, V.; Mazzaferro, S.; Evenepoel, P.; Bover, J.; Apetrii, M.; et al. Bone and mineral disorders in chronic kidney disease: Implications for cardiovascular health and ageing in the general population. *Lancet Diabetes Endocrinol.* 2018, 6, 319–331.
4. Clarke, B. Normal Bone Anatomy and Physiology. *Clin. J. Am. Soc. Nephrol.* 2008, 3 (Suppl. 3), S131–S139.
5. Jevtic, V. Imaging of renal osteodystrophy. *Eur. J. Radiol.* 2003, 46, 85–95.
6. Siakallis, L.; Tziakouri-Shiakalli, C.; Georgiades, C.S. Erratum to “Amyloidosis: Review and Imaging Findings” [Seminars in Ultrasound, CT, and MRI 2014;35(3):225-239]. *Semin. Ultrasound CT MRI* 2015, 36, 216.
7. Kiss, E.; Keusch, G.; Zanetti, M.; Jung, T.; Schwarz, A.; Schocke, M.; Jaschke, W.; Czermak, B.V. Dialysis-Related Amyloidosis Revisited. *Am. J. Roentgenol.* 2005, 185, 1460–1467.
8. Cummings, S.R.; Bates, D.; Black, D.M. Clinical use of bone densitometry: Scientific review. *JAMA* 2002, 288, 1889–1897.
9. Silva, B.C.; Leslie, W.D.; Resch, H.; Lamy, O.; Lesnyak, O.; Binkley, N.; McCloskey, E.V.; Kanis, J.A.; Bilezikian, J.P. Trabecular Bone Score: A Noninvasive Analytical Method Based Upon the DXA Image. *J. Bone Miner. Res.* 2014, 29, 518–530.
10. Yavropoulou, M.P.; Vaios, V.; Pikilidou, M.; Chrysosgonidis, I.; Sachinidou, M.; Tournis, S.; Makris, K.; Kotsa, K.; Daniilidis, M.; Haritanti, A.; et al. Bone Quality Assessment as Measured by Trabecular Bone Score in Patients With End-Stage Renal Disease on Dialysis. *J. Clin. Densitom.* 2017, 20, 490–497.
11. Hayashi, Y.; Yamamoto, K.; Fukunaga, M.; Ishibashi, T.; Takahashi, K.; Nishii, Y. Assessment of bone mass by image analysis of metacarpal bone roentgenograms: A quantitative digital image processing (DIP) method. *Radiat. Med.* 1990, 8, 173–178.
12. Ross, P.D. Radiographic absorptiometry for measuring bone mass. *Osteoporos. Int.* 1997, 7 (Suppl. 3), S103–S107.
13. Dey, A.; McCloskey, E.V.; Taube, T.; Cox, R.; Pande, K.C.; Ashford, R.U.; Forster, M.; de Takats, D.; Kanis, J.A. Metacarpal Morphometry Using a Semi-automated Technique in the Assessment of Osteoporosis and Vertebral Fracture Risk. *Osteoporos. Int.* 2000, 11, 953–958.
14. Nakagawa, Y.; Komaba, H.; Hamano, N.; Wada, T.; Hida, M.; Suga, T.; Kakuta, T.; Fukagawa, M. Metacarpal bone mineral density by radiographic absorptiometry predicts fracture risk in patients

undergoing maintenance hemodialysis. *Kidney Int.* 2020, 98, 970–978.

15. Aaltonen, L.; Koivuviita, N.; Seppänen, M.; Tong, X.; Kröger, H.; Löyttyniemi, E.; Metsärinne, K. Correlation between ¹⁸F-Sodium Fluoride positron emission tomography and bone histomorphometry in dialysis patients. *Bone* 2020, 134, 115267.
16. Messa, C.; Goodman, W.G.; Hoh, C.K.; Choi, Y.; Nissenson, A.R.; Salusky, I.B.; Phelps, M.E.; Hawkins, R.A. Bone metabolic activity measured with positron emission tomography and [¹⁸F]fluoride ion in renal osteodystrophy: Correlation with bone histomorphometry. *J. Clin. Endocrinol. Metab.* 1993, 77, 949–955.
17. Wittich, A.; Vega, E.; Casco, C.; Marini, A.; Forlano, C.; Segovia, F.; Nadal, M.; Mautalen, C. Ultrasound Velocity of the Tibia in Patients on Hemodialysis. *J. Clin. Densitom.* 1998, 1, 157–163.
18. Goldenstein, P.T.; Jamal, S.A.; Moyses, R.M. Fractures in chronic kidney disease: Pursuing the best screening and management. *Curr. Opin. Nephrol. Hypertens.* 2015, 24, 317–323.

Retrieved from <https://encyclopedia.pub/entry/history/show/26040>